Available online at www.sciencedirect.com
SCIENCE DIRECT®
Journal of Molecular Structure 657 (2003) 191–198
Journal of MOLECULAR STRUCTURE
www.elsevier.com/locate/molstruc

Structural characterization of two novel potential anticholinesterasic agents

Paulo R. Oliveira[a], Franciele Wiectzycosky[b], Ernani A. Basso[b,*], Regina A.C. Gonçalves[c], Rodrigo M. Pontes[b]

[a]*Instituto de Química, Universidade Estadual de Campinas, Caixa Postal 6154, 13083-970 Campinas, São Paulo, Brazil*
[b]*Departamento de Química, Universidade Estadual de Maringá, Av. Colombo, 5790, 87020-900, Maringá-PR, Brazil*
[c]*Departamento de Farmácia e Farmacologia, Universidade Estadual de Maringá, Av. Colombo, 5790, 87020-900, Maringá-PR, Brazil*

Received 25 April 2003; revised 30 May 2003; accepted 30 May 2003

Abstract

Two novel compounds with possible anticholinesterase activity have been synthesized containing a carbamate and a dimethylamine group in 1,2-positions of a cyclohexane ring (*cis* and *trans* isomers). Conformer populations were established by a combination of NMR ^{1}H coupling constant analysis and DFT (B3LYP/6-311 + G(d,p)) calculations. ^{13}C chemical shifts were calculated in order to confirm signal attributions. The *cis* isomer adopts a conformation in which the carbamate group lies at the axial position (>99%), whereas the *trans* isomer adopts a diequatorial arrangement (98%). These preferences have been explained in terms of *syn*-1,3-diaxial interactions of the individual groups.

Keywords: Anticholinesterasic; Synthesis; Conformational analysis; Nuclear magnetic resonance; Theoretical calculations

1. Introduction

Anticholinesterasic compounds are drugs that inhibit the action of the acetycholinesterase enzyme (AChE), and are important in the treatment of illness such as myasthenia gravis and Alzheimer's disease [1–3]. The role of an anticholinesterase inhibitor is to bind to AChE, reducing the enzyme degradation of the neurotransmitter acetylcholine (ACh).

Several compounds have been developed with this end, and ongoing research has been aimed at obtaining more potent, selective and safe AChE inhibitors [1–6]. Two structural features are common to most of the molecules classified as anticholinesterasic agents, viz. an alkylammonium group and an oxygen atom 4.4–5.9 Å apart. In some cases, the alkylammonium group may be replaced by a tertiary amine nitrogen, which can be positively charged at physiological pH [2].

Our laboratory has synthesized two potential antycholinesterasic agents, namely *cis*-2-*N*,*N*-dimethylaminecyclohexyl 1-*N*′,*N*′-dimethylcarbamate (**1**; Fig. 1a) and *trans*-2-*N*,*N*-dimethylaminecyclohexyl 1-*N*′,*N*′-dimethylcarbamate (**2**; Fig. 1b). Each of them has two possible conformations generated by the interconversion of the cyclohexane ring.

* Corresponding author. Tel.: +55-44-261-4332; fax: +55-44-263-5784.
E-mail address: eabasso@uem.br (E.A. Basso).

0022-2860/03/$ - see front matter © 2003 Elsevier B.V. All rights reserved.
doi:10.1016/S0022-2860(03)00367-3

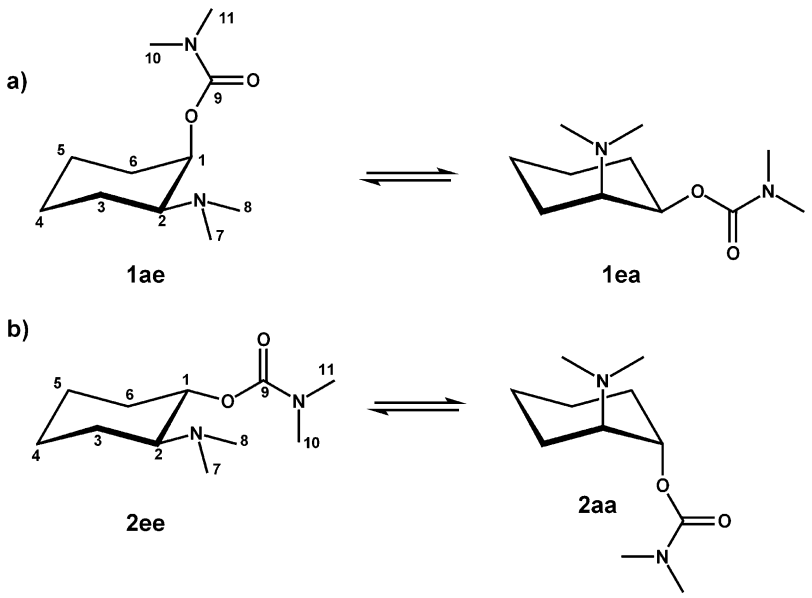

Fig. 1. Conformational equilibrium for: (a) **1**; and (b) **2**.

Pharmacological studies for these compounds are being conducted and the results will be published elsewhere. The main purpose of this article is to give a description of their molecular structure, including a study of the conformational preference by means of nuclear magnetic resonance (NMR) spectroscopy and theoretical calculations. The knowledge of structural features is of fundamental importance in the understanding of the biological behavior.

2. Experimental

2.1. Compound preparations

Compounds **1** and **2** were synthesized following the route in Fig. 2. The individual steps are well described in the literature. Cyclohexanone (**3**) was reacted with bromine to obtain 2-bromocyclohexanone (**4**) [7], which was placed in an autoclave with

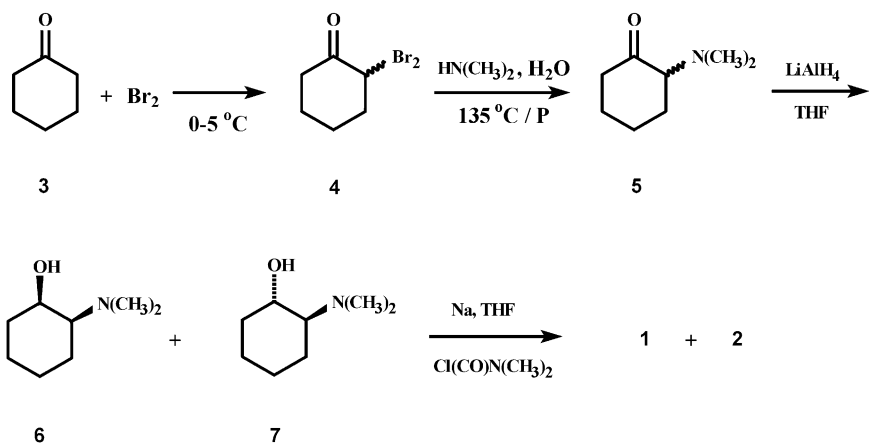

Fig. 2. Synthetic route for obtaining of compounds **1** and **2**.

Table 1
Boiling points and yieldings for the compounds involved in the synthetic route of **1** and **2**

Compound	Boiling point (°C)/*P* (Torr)	Yield%
1,2	101–102/1.5	57
3	154/760	–
4	52–53/1.0	56
5	53–54/1.2	53
6,7	55–57/1.6	77

N,*N*-dimethylamine solution to give 2-*N*,*N*-dimethylaminecyclohexanone (**5**) [8]. Reduction of **5** with lithium aluminum hydride [9] gave a mixture of *cis* and *trans* (25:75) 2-*N*,*N*-dimethylaminecyclohexanol (**6** and **7**, respectively) that were subsequently reacted with *N*,*N*-dimethylcarbamyl chloride to obtain the target compounds [10]. The *cis* and *trans* isomers were isolated from each other through elution of the reaction products in a silica column (acetone/ethanol 7:3). The data regarding the synthetic route are summarized in Table 1.

2.2. NMR measurements

NMR spectra were acquired on a Varian Gemini 2000/300 spectrometer. $CDCl_3$ solutions were employed to obtain the spectra used for signal attribution. Samples were prepared by placing ca. 50 mg of the compound in 0.5 ml of the solvent in a 5 mm o.d. NMR tube. Typical conditions for ^{13}C spectra were sweep width of 18 kHz, pulse angle of 30°, 256 scan and 1 s delay time. Spectra were stored in 32 K data blocks. For ^{1}H spectra, sweep width was typically 4000 Hz, pulse angle of 45°, 62 scans, 1 s delay time and 16 K of data points. Deuterated solvents were obtained commercially and used as received.

2.3. Calculations

The GAUSSIAN 98 package [11] was used to carry out all the calculation. DFT was applied with Becke's three-parameter hybrid method [12] and correlation functional of Lee, Yang and Parr (B3LYP) [13], in conjunction with the 6-311 + G(d,p) basis set for geometry optimization and 6-31G(d,p) for shielding tensors calculations. Geometries were optimized and confirmed as minima by frequencies calculations, and zero-point energies were scaled by 0.9806 [14]. The optimized structures were submitted to magnetic properties calculations using the GIAO method [15]. Comparison with experiment (δ) was accomplished by calculating the absolute shielding for tetramethylsilane (TMS) and using the following equation

$$\delta(C_i) = \sigma_{TMS}(C) - \sigma(C_i)$$

where $\sigma_{TMS}(C)$ is the TMS absolute shielding and $\sigma(C_i)$ is the absolute shielding for nucleus *i*.

3. Results and discussion

3.1. Assignments and conformational preference by ^{1}H spectra

Signal assignments were accomplished by taking into account ^{1}H coupling constants, when possible, and combining these data with DEPT and HETCOR experiments (Tables 2 and 3). Additionally, we have evaluated ^{13}C chemical shifts through DFT-B3LYP/6-31G(d,p) calculations. The calculated chemical shifts are, in most of the cases, larger than the observed ones, which may be due the fact that

Table 2
^{1}H NMR chemical shifts for compounds **1** and **2**

	H-1	H-2	H-3(eq)[a]	H-3(ax)[a]	H-4(eq)[a]	H-4(ax)[a]	H-5(eq)[a]	H-5(ax)[a]	H-6(eq)[a]	H-6(ax)[a]	H-7/H-8	H-10	H-11
1	5.30	2.16	1.78	1.68	1.82	1.32	1.47	1.47	1.93	1.38	2.33	2.93	2.95
2	4.77	2.50	1.82	1.34	1.72	1.20	1.66	1.28	2.03	1.28	2.35	2.92	2.92

Spectrum acquired in $CDCl_3$ solution; in ppm downfield from TMS.
[a] eq and ax refers to equatorial and axial hydrogens, respectively, in the cyclohexane ring.

Table 3
^{13}C Experimental and calculated (in parenthesis) chemical shifts for compounds **1** and **2**

	C-1	C-2	C-3	C-4	C-5	C-6	C-7/C-8[a]	C-9	C-10	C-11
1	70.01	65.81	25.65	25.38	20.29	30.46	42.64	156.26	36.00	36.41
	(71.44)	(70.49)	(31.18)	(30.30)	(25.95)	(35.16)	(45.64)	(149.75)	(37.56)	(38.41)
2	73.79	66.06	26.00	24.71	24.10	32.19	41.34	156.56	36.04	36.45
	(74.02)	(72.07)	(26.01)	(30.20)	(29.80)	(37.29)	(43.09)	(149.50)	(36.99)	(37.87)

Computed at B3LYP/6-31G(d,p); spectra acquired in $CDCl_3$ solution; in ppm downfield from TMS.
[a] These carbons appear as a single peak and the calculated values were obtained by averaging over the values of each carbon.

calculations do not take into account solvent effects. Nevertheless, the relative positions are sufficient to help in the assignments of some dubious signals. This is the case, for instance, of nucleus 10 and 11 (Fig. 1). The attribution of these peaks could be performed through ASIS (aromatic solvent induced shift) experiments on the ^1H spectra [16,17], but this requires that the peaks present a reasonable separation, which is not the case. In this way, we have attributed C-10 and C-11 with the help of the calculated values. In compound **1**, H-10 and H-11 show a slightly separation (0.02 ppm), but the HETCOR spectra was not enough resolved to allow a direct correlation with C-10 and C-11. Therefore, we have attributed H-10 and H-11 by admitting that they follow the same pattern of the ^{13}C spectra.

Conformational preference may be assessed by analyzing the information contained in the coupling patterns of the cyclohexane hydrogens [10,18]. Unfortunately, most of these signals are involved in second order spectra, which makes difficult to identify the individual couplings. However, the proton close to the oxygen atom (H-1) appears at sufficient high field to allow an individual analysis. Fig. 3 depicts this signal for **1** and **2**. Notice the difference in shape; while the couplings are clear for **2**, for **1**, it is not possible to identify any splitting pattern.

It is a well-known fact that proton vicinal couplings depend markedly on the dihedral angle (ω) between the two C–H bonds [19]. In this way, for ω close to 180°, the coupling constant presents a value of about 10 Hz, while for ω close to 60°, its value is approximately 5 Hz. In the case of **1**, it is not possible to identify any individual coupling for H-1, so we have measured the *W* value, i.e. the signal width at half height, which measures the sum of vicinal couplings (with H-6 and H-2) plus any long-range couplings. The value so obtained is 13 Hz, in accordance to what is expected by taking into account the individual splittings resulting from an equatorial position. If H-1 were in an axial arrangement, the total coupling (J_T), i.e. the value obtained by measuring

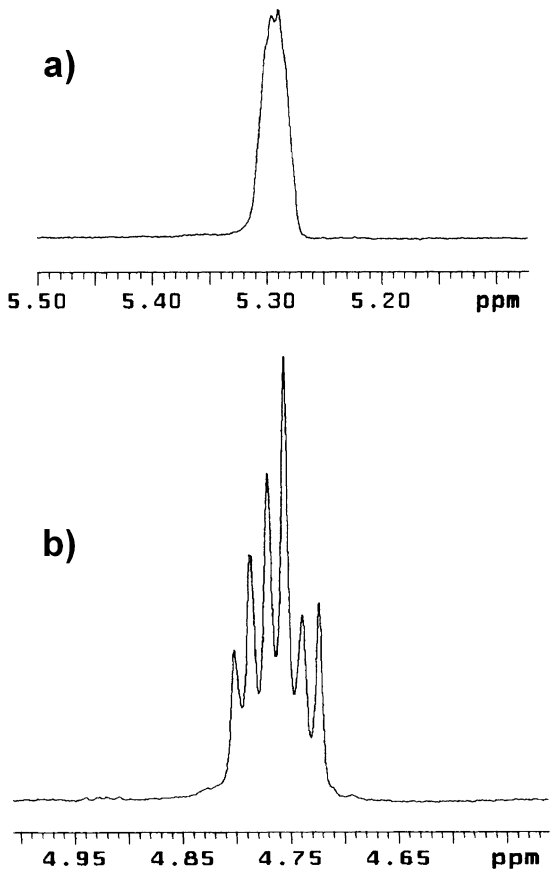

Fig. 3. ^1H spectrum for the H-1 region (in $CDCl_3$): (a) **1**; (b) **2**.

Table 4
Selected structural parameters for the conformers of compounds **1** and **2** (bond lengths in Å, bond angles in °, dipole moments in debyes and energies in hartrees)

	1ae	**1ea**	**2ee**	**2aa**
Bond lengths				
$r(C_1-O)$	1.450	1.443	1.445	1.457
$r(C_9=O)$	1.219	1.219	1.219	1.218
$r(C_9-O)$	1.359	1.357	1.359	1.361
$r(C_9-N)$	1.366	1.366	1.365	1.366
$r(N-C_{10})$	1.456	1.456	1.455	1.456
$r(N-C_{11})$	1.455	1.454	1.454	1.455
$r(C_2-N)$	1.473	1.471	1.469	1.479
$r(C_7-N)$	1.460	1.456	1.459	1.460
$r(C_8-N)$	1.464	1.455	1.455	1.464
$r(C_1-C_2)$	1.546	1.555	1.540	1.550
$r(C_1-C_6)$	1.530	1.528	1.530	1.528
$r(C_2-C_3)$	1.540	1.556	1.548	1.541
$r(C_5-C_6)$	1.532	1.534	1.534	1.534
$r(C_3-C_4)$	1.537	1.537	1.534	1.536
$r(C_4-C_5)$	1.532	1.533	1.533	1.543
Bond angles				
$\angle(C_1-O-C_9)$	117.7	117.0	117.8	116.9
$\angle(O-C_9-N)$	111.7	111.9	117.7	111.8
$\angle(O-C_9=O)$	123.9	123.5	123.9	123.6
$\angle(C_9-N-C_{10})$	123.8	124.0	124.5	124.3
$\angle(C_9-N-C_{11})$	118.7	118.8	119.1	119.0
$\angle(O-C_1-C_2)$	108.8	112.2	109.2	108.6
$\angle(O-C_1-C_6)$	108.1	108.2	107.1	107.6
$\angle(C_1-C_2-N)$	111.1	114.4	111.8	109.2
$\angle(C_2-N-C_7)$	114.2	112.7	116.1	114.5
$\angle(C_2-N-C_8)$	112.2	118.7	113.5	111.8
Dihedral angles				
$\phi(C_1-O-C_9=O)$	5.1	−5.1	−8.4	−1.2
$\phi(C_{10}-N-C_9=O)$	−173.3	174.4	177.8	−178.7
$\phi(C_{11}-N-C_9=O)$	−5.7	4.3	−0.5	−3.5
$\phi(O-C_1-C_2-N)$	−61.7	−35.3	57.5	−168.4
$\phi(C_1-C_2-N-C_7)$	168.2	152.1	−155.2	−163.4
$\phi(C_1-C_2-N-C_8)$	−66.1	−75.7	73.4	72.1
$\phi(O-C_1-C_2-C_3)$	64.7	−169.3	−173.1	66.6
$\phi(O-C_1-C_6-C_5)$	−64.8	178.3	175.1	−66.6
μ	2.44	2.20	2.31	2.36
E	−692.580026	−692.573382	−692.582630	−692.579147
ZPE[a]	0.323663	0.323511	0.323218	0.323622

Computed at the B3LYP/6-311 + G(d,p).
[a] Zero-point energy correction scaled by 0.9806.

the distance between the tops of the extreme peaks, should be close to 20 Hz.

Another evidence of the conformational preference of **1** can be obtained by considering the H-2 signal. The total coupling constant should present a value of about 13 Hz if H-1 were in the equatorial position (conformation **1ea**, Fig. 1), but the observed value is 17.55 Hz, in accordance to what is expected by analyzing the couplings resulting from an axial position. Therefore, we conclude that **1ae** is

the predominant conformer of **1**. Theoretical calculations corroborate with this preference, as will be discussed in Section 3.3.

A similar analysis may be conducted for compound **2**. The H-1 signal (Fig. 3b) presents a well-resolved shape and, in addition to W, we were able to measure the individual couplings and J_T. The values so obtained are $W = 27.5$ Hz, $J(\text{H-1}_{(ax)}, \text{H-2}_{(ax)}) = 9.75$ Hz, $J(\text{H-1}_{(ax)}, \text{H-6}_{(ax)}) = 9.75$ Hz, $J(\text{H-1}_{(ax)}, \text{H-6}_{(eq)}) = 4.5$ Hz, $J_T = 24$ Hz (the estimated value is 25 Hz). These values indicate that H-1 makes two axial coupling, which is possible only in the case of conformation **2ee**. Similarly, the H-2 peak presents a value of 24.75 Hz for J_T, for an estimation of 25 Hz.

3.2. Theoretical analysis of the conformational equilibrium

Table 4 presents the geometrical parameters for **1** and **2**, and Fig. 4 shows the optimized structures. In Table 5 we have listed the relative energies and calculated populations (n_i) for each conformer. These

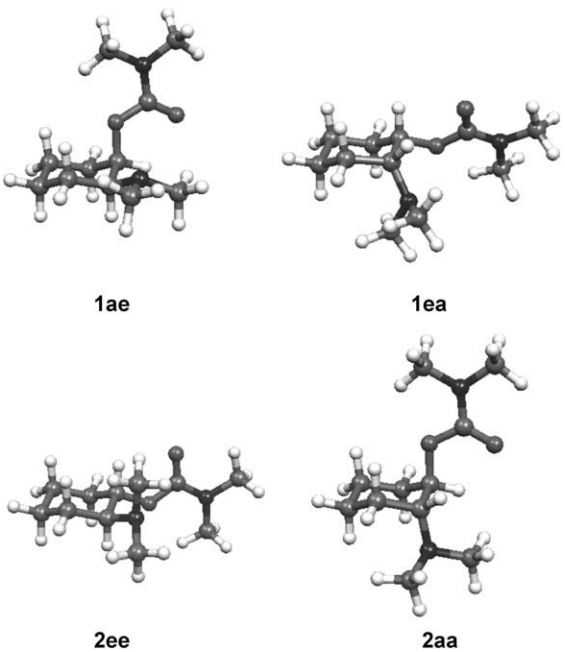

Fig. 4. Optimized structures for the conformers of compounds **1** and **2**.

Table 5
Relative energies (in kcal mol^{-1}) and mole fractions (n) for the conformers of compounds **1** and **2**

Level	$E_{1ea} - E_{1ae}$ [a]	$E_{2aa} - E_{2ee}$ [a]	n_{1ae}	n_{2ee}
HF/STO-3G	3.71	2.41	0.998	0.983
HF/3-21G	5.24	1.95	0.999	0.964
HF/6-31G(d,p)	4.28	2.98	0.999	0.994
B3LYP/6-31G(d,p)	4.19	2.54	0.999	0.986
B3LYP/6-311 + G(d,p)	4.07	2.44	0.999	0.984

[a] Including ZPE corrections.

values were obtained by approximating the Gibbs energy difference (ΔG^0) by the enthalpy difference at 0 K (ΔH_0^0)—that includes electronic, nuclear repulsion and zero-point energies—and using van't Hoff equation

$$\Delta G^0 = -RT \ln K$$

where K ($= n_{ax}/n_{eq}$) is the equilibrium constant, R ($= 1.98722$ cal K^{-1} mol^{-1}) is the gas constant and T (set as 298.15 K) is the absolute temperature.

For comparison, conformer populations were determined at five different levels of theory. All of them agree that **1ae** and **2ee** represent almost all the compound population, even when small basis set are used. These preferences may be explained in terms of steric repulsion, as follows.

Fig. 5 depicts the repulsion between the individual substituents and the hydrogens at 1 and 3 arrangements (*syn*-1,3-diaxial interactions). When the substituents adopt equatorial positions, these repulsions are avoided. Guided by this principle, we can understand the conformational preference in **2** by noting that in the conformer **2aa**, the two substituents occupy axial positions, i.e. *syn*-1,3-diaxial interactions predominate. On the contrary, in **2ee**, both substituents occupy equatorial positions, and, consequently, steric repulsion is minimized.

Compound **1** requires some more considerations. In this case, both conformers possess an axial and an equatorial group, and we are lead to ask why **1ea** is so unstable relative to **1ae**. To answer this question, we must consider the conformational equilibrium of the individual substituents in the cyclohexane ring. The experimental proportions of the equatorial

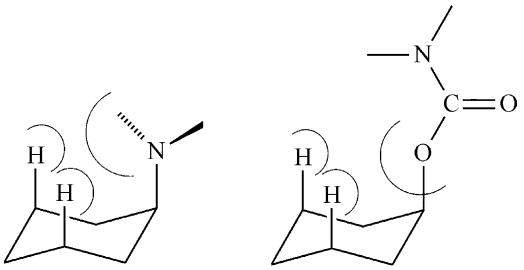

Fig. 5. Steric interactions between the studied substituents and the hydrogens at 1 and 3 arrangements.

Table 6
Distances between the amine (or ammonium) nitrogen (N_{am}) and the ester (O_{ester}) or carbonyl (O_{carb}) oxygen (in Å)

	$r(N_{am}\cdots O_{ester})$	$r(N_{am}\cdots O_{carb})$
Acetylcholine	3.737	5.140
1ae	2.908	3.657
1ea	2.829	3.699
2ee	2.877	3.502
2aa	3.727	4.275

Computed at the B3LYP/6-311 + G(d,p)

conformer in these equilibriums are 80% [10,20] and 93% [21] for $-O(C{=}O)N(CH_3)_2$ and $-N(CH_3)_2$, respectively. From this, it is clear that the individual behavior prevails when the two groups are combined. Inspection of Fig. 5 clearly shows that the carbamate group has a larger volume, but the 1,3-diaxial interactions involve mainly the 'ester' oxygen, since the other atoms are relatively distant from the ring. On the other hand, the entire amine group is close enough for the cyclohexane ring to cause a greater repulsion.

3.3. Comparison with acetylcholine

ACh is one of the benchmark molecules used for assessing antycholinesterase activity. The interaction of a drug with the enzyme active site depends crucially on the distance between the amine nitrogen and the carbamate oxygens. Based on such distances, the actions of ACh have been divided into two categories, nicotinic and muscarinic [2], by analogy with the effects of nicotine and muscarine. Beers and Reich [2] have proposed that the specific binding of nicotinic agents to their binding sites depends on Coulombic interactions involving the amine nitrogen, and on a hydrogen bond formed with an acceptor group disposed at approximately 5.9 Å from the nitrogen ($r(N_{am}\cdots O_{carb})$). In muscarinic agents, this distance is approximately 4.4 Å ($r(N_{am}\cdots O_{ester})$). Actually, the distances used by the authors were defined as the distance from the nitrogen atom to a point on the van der Waals surface of the electron donor oxygen. Space-fill models were used for that study. For the present investigation, we opt for comparing the distances in compounds **1** and **2** with those obtained directly from density functional calculation for ACh. In Table 6 we list the distances so obtained after geometry optimization for ACh at the same level of theory used for **1** and **2**. Fig. 6 depicts the optimized structure for ACh.

According to Table 6, the predominant conformers, i.e. **1ae** and **1ea**, have expressively different atom distances relative to ACh, which, in principle, suggests an absence of activity for these compounds. Notice, however, the distances for the **2aa** conformer. In this case, $r(N_{am}\cdots O_{ester})$ is very close to that in ACh, which could be used, in principle, to classify this conformer as a muscarinic agent. Nevertheless, **2aa** is practically absent in the conformational equilibrium of **2** (the energy difference between **2ee** and **2aa** is 2.44 kcal mol^{-1}, see Table 5). The energy of binding

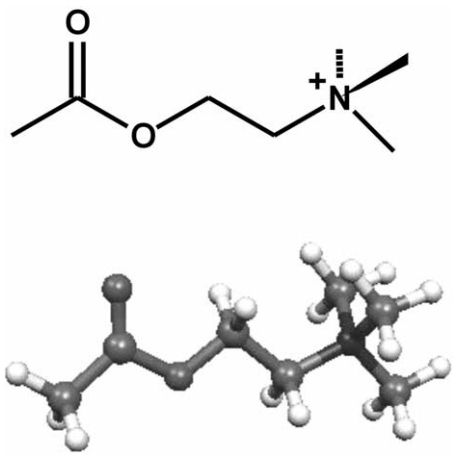

Fig. 6. Structural representation (top) and optimized structure (bottom) for acetylcholine.

of a series of AChE inhibitors was found to be essentially constant, viz. 4.2 kcal mol^{-1} [22]; taking this fact into account, we see that the binding of **2aa** with AChE could be able to displace the equilibrium between **2ee** and **2aa** in the direction of the latter.

Finally, bond rotations or ring torsions could recover the differences in distances (that are about 0.8 Å for the nitrogen and ester oxygen) between ACh and the compounds under study. How effectively the binding process can accomplish this, experiments will show.

Acknowledgements

This research was supported by Fundação Araucária (grant number: 325) and Fundação de Amparo à Pesquisa do Estado de São Paulo (FAPESP; grant number: 07692-5). CAPES (Coordenação de Aperfeiçoamento de Pessoal de Nível Superior) is acknowledged for scholarships to P.R.O., F.W. and R.M.P. The authors also thanks to CENAPAD-SP (Centro Nacional de Processamento de Alto Desempenho de São Paulo) for the computer facilities.

References

[1] S. Roman, N.M. Vivas, A. Badia, M.V. Clos, Neurosci. Lett. 325 (2002) 103.
[2] W.H. Beers, E. Reich, Nature 228 (1970) 917.
[3] W.C. Bowman, Anesth. Analg. 59 (1980) 935.
[4] E. Narimatsu, Y. Nakayama, S. Sumita, H. Iwasaki, N. Fujimura, K. Satoh, A. Namiki, Acta Anaesth. Scand. 43 (1999) 196.
[5] J.B. Kay, J.B. Robinson, B. Cox, D. Polkonjak, J. Pharm. Pharmacol. 22 (1970) 214.
[6] M.F. Braga, E.G. Rowan, A.L. Harvey, W.C. Bowman, Br. J. Anaesth. 70 (1993) 405.
[7] J. Allinger, N.L. Allinger, Tetrahedron 2 (1958) 64.
[8] M. Mousseron, J. Jullian, Y. Jolchine, Bull. Soc. Chem. Fr. 19 (1952) 757.
[9] C. Bernard, M.T. Maurette, A. Latters, Bull. Soc. Chem. Fr. 1/2 (1976) 145.
[10] E.A. Basso, P.R. Oliveira, J. Caetano, I.T.A. Schuquel, J. Braz. Chem. Soc. 12 (2001) 215.
[11] M.J. Frisch, G.W. Trucks, H.B. Schlegel, G.E. Scuseria, M.A. Robb, J.R. Cheeseman, V.G. Zakrzewski, J.A. Montgomery, Jr, R.E. Stratmann, J.C. Burant, S. Dapprich, J.M. Millam, A.D. Daniels, K.N. Kudin, M.C. Strain, O. Farkas, J. Tomasi, V. Barone, M. Cossi, R. Cammi, B. Mennucci, C. Pomelli, C. Adamo, S. Clifford, J. Ochterski, G.A. Petersson, P.Y. Ayala, Q. Cui, K. Morokuma, D.K. Malick, A.D. Rabuck, K. Raghavachari, J.B. Foresman, J. Cioslowski, J.V. Ortiz, A.G. Baboul, B.B. Stefanov, G. Liu, A. Liashenko, P. Piskorz, I. Komaromi, R. Gomperts, R.L. Martin, D.J. Fox, T. Keith, M.A. Al-Laham, C.Y. Peng, A. Nanayakkara, M. Challacombe, P.M.W. Gill, B. Johnson, W. Chen, M.W. Wong, J.L. Andres, C. Gonzalez, M. Head-Gordon, E.S. Replogle, J.A. Pople, GAUSSIAN 98 (Revision A.9), Gaussian, Inc., Pittsburgh PA, 1998.
[12] A.D. Becke, J. Chem. Phys. 98 (1993) 1372.
[13] C. Lee, W. Yang, R.G. Parr, Phys. Rev. B 37 (1988) 785.
[14] A.P. Scott, L. Radon, J. Phys. Chem. 100 (1996) 16502.
[15] J.R. Cheeseman, G.W. Trucks, T.A. Keith, M.J. Frish, J. Chem. Phys. 104 (1996) 5497.
[16] B.B. Wayland, R.S. Drago, H.F. Henneike, J. Am. Chem. Soc. 88 (1966) 2455.
[17] C.F. Tormena, R. Rittner, R.J. Abraham, E.A. Basso, R.M. Pontes, J. Chem. Soc. Perkin Trans. 2 (2000) 2054.
[18] E.A. Basso, C. Kaiser, R. Rittner, J.B. Lambert, J. Org. Chem. 58 (1993) 7865.
[19] M. Karplus, J. Am. Chem. Soc. 85 (1963) 2870.
[20] E.A. Basso, R.M. Pontes, J. Mol. Struct. (THEOCHEM) 594 (2002) 199.
[21] H. Booth, M.L. Josefowicz, J. Chem. Soc. Perkin Trans. 2 (1976) 895.
[22] B. Belleau, J.L. Lavoie, Can. J. Biochem. 46 (1968) 1397.